



Transactions, SMiRT-25
Charlotte, NC, USA, August 4-9, 2019
Division II Paper ID 786

MODELING OF NATURAL CRACK GROWTH WITH XFEM

Yihai Shi¹, Xinjian Duan¹, Min Wang¹

¹ Candu Energy Inc., Mississauga, Ontario, Canada (xinjian.duan@snclavalin.com)

INTRODUCTION

In the CANDU reactor, dissimilar metal welds (DMWs) are present in some of the outlet feeders. Operating experience from pressurized water reactors (PWRs) piping butt welds suggests that such dissimilar metal welds (DMWs) may be susceptible to primary water stress corrosion cracking (PWSCC) especially at the high residual stress locations, such as weld repair or start/stop. Natural crack growth behavior refers to the prediction of crack growth using the stress intensity factor determined at points along the entire crack front instead of conventionally using only the deepest and surface points to grow semi-elliptical crack fronts. This approach is still an approximation but a closer approximation to the “natural” real case than alternative methods and has been adopted by the industry in modeling the crack growth simulation [1-6]. The particularly advantage is that the crack front shapes and the time taken better represent the response to a complex and changing stress field. The stress intensity factor (SIF) solutions are widely used in fracture analysis of crack structures. Most of the recently developed SIF solutions are based on finite element analysis [2-6]. For these solutions, the conventional focused crack-tip meshes were employed to calculate the SIF values using domain integral. The conventional focused meshes brings an extreme challenge to model the continuous crack growth from finite element modeling perspective, due to the factor that the focused mesh in the crack front has to be updated every single step. In the past the mesh generator (such as AFEA by Emc² [1]) has been developed to serve this purpose and successfully to model the natural crack growth in the piping model.

In this paper, a more generic XFEM approach in calculating SIF is adopted and detailed techniques of using XFEM in modeling natural crack growth are discussed along with some benchmark against the works done through the AFEA approach.

Extended Finite Element Method (XFEM)

Since the crack growth was based on the stress intensity factor (K_I), following [1], a simple elastic material model is used for crack growth predictions. In this work, K_I solutions were calculated using XFEM in ABAQUS [7]. The concept of partition of unity in XFEM allows the presence of discontinuities in an element by enriching degrees of freedom with special displacement function. It does not require the mesh to match the geometry of the discontinuities. The XFEM methodology incorporated in ABAQUS uses additional terms in the displacement function to model the presence of crack. A jump function with nodal enrichment functions, along with asymptotic crack-tip functions with corresponding modal enrichment degree of freedom vector is used.

$$\mathbf{u} = \sum_{i=1}^N N_i(\mathbf{x}) [\mathbf{u}_i + \mathbf{H}(\mathbf{x}) \mathbf{a}_i + \sum_{\alpha=1}^4 F_{\alpha}(\mathbf{x}) \mathbf{b}_i^{\alpha}] \quad (1)$$

where, \mathbf{u} is the displacement vector, $N_i(\mathbf{x})$ are the shape function, $\mathbf{H}(\mathbf{x})$ is a Jump function, \mathbf{a}_i is nodal enriched degree of freedom vector, $F_{\alpha}(\mathbf{x})$ is asymptotic crack-tip functions, \mathbf{b}_i^{α} is the nodal enriched degree of freedom vectors.

The conventional method requires a mesh that conforms to the crack geometry, typically with a very detailed focus on the crack front as shown in Figure 1(a). The focused mesh needs very detailed domain partition near the crack front and pre-process is very tedious and time-consuming. For some

arbitrary cracks, meshing becomes extremely challenging or even impossible. The XFEM-based approach does not require the mesh to explicitly match the geometry of the crack. Figure 1(b) shows the crack model with XFEM approach. With respect to the element shape, the primary difference between the methods is that XFEM does not require the construction of collapsed elements around the crack front. Regularly shaped elements can be used, as a result the specification of an initial crack is greatly simplified. The automatic natural crack growth modeling also becomes possible.

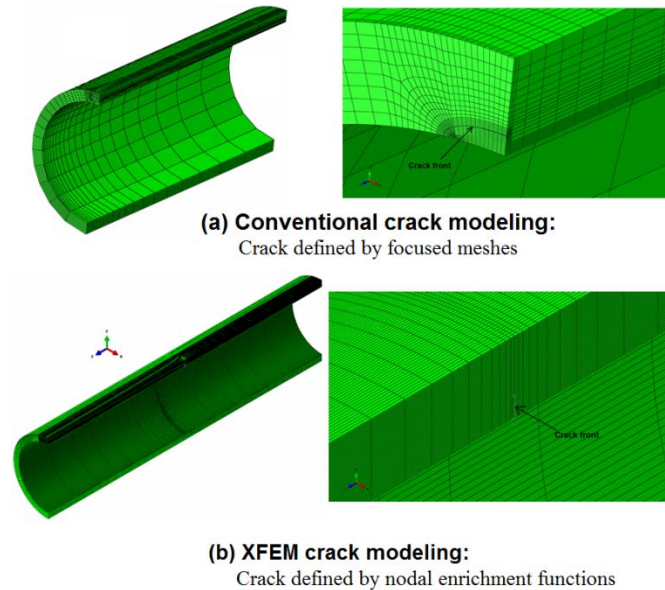


Figure 1 Crack front (surface) modeling, (a) conventional approach. (b) XFEM approach

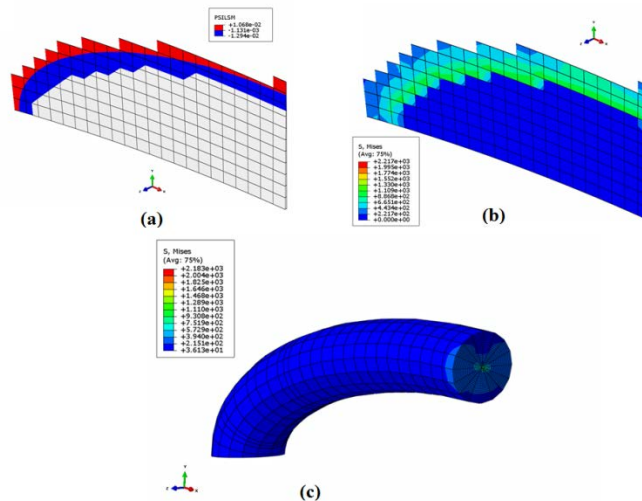


Figure 2 Crack modeling with XFEM, (a) crack PSILSM iso-surfaces of XFEM meshes showing the crack; (b) stress distribution along the crack front after loading; (c) sub-model in ABAQUS calculating the K and J values

In ABAQUS, XFEM crack can be explicitly displayed through plotting distant variables in an iso-surface model as shown in Figure 2(a) and (b). In evaluating the contour integral, ABAQUS constructed an internal, independent sub-model around the crack front line shown in Figure 2(c). Contour integral

results are obtained from this sub-model using the conventional technique. Visualizing this mesh can help to further understand how the contour integral is calculated.

Crack Growth Rate

In the present work, ABAQUS is employed to calculate the K_I values at each node along the crack front. These results are then used to determine the amount of crack growth at each location (i.e., each crack front node). The crack growth direction is defined as the direction normal to the crack front at each nodal location. The MRP-115 crack growth rate model for alloy 182 (rather than alloy 600), which is a function of K_I and temperature, was adopted for conservatism purposes because, based on Reference [8], Alloy 182 has the largest growth rate compared with alloy82 and alloy 600.

$$\dot{a} = \exp \left[-\frac{Q_g}{R} \left(\frac{1}{T} - \frac{1}{T_{ref}} \right) \right] \gamma f_{weld} f_{alloy} f_{orient} K^\beta \quad (2)$$

where, \dot{a} is crack growth rate at temperature T in m/s; Q_g is thermal activation energy for crack growth = 130kJ/mole; R is universal gas constant = 8.134x10⁻³ kJ/mole-K; T absolute operating temperature at the crack location in K; T_{ref} absolute operating temperature to normalize data=598.15K; γ power law constant =9.83x10⁻¹³; f_{alloy} 1.0 for alloy 182; f_{orient} 1.0 for growth parallel to dendrite solidification direction; β exponent=1.6.

The cumulative distribution of the weld factor (f_{weld}) is shown in Figure 3. In this work, the 75th percentile value of f_{weld} was used. Note that this value (75th percentile) was also used by USNRC in Reference [9] and US nuclear industry in Reference [10].

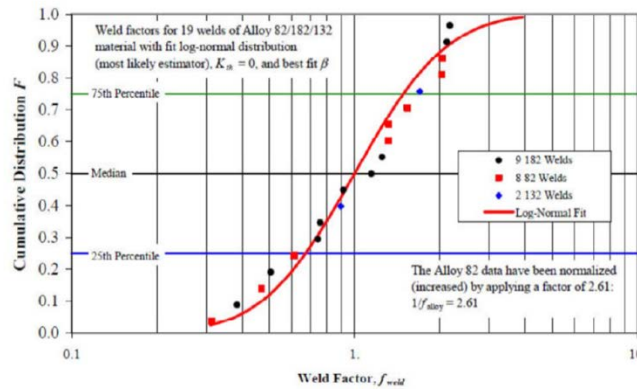


Figure 3 Weld factor for alloy 182 crack growth rates

In the current model, the crack growth is controlled by two parameters, i.e., time increment and maximum crack growth length. The time increment, along with the crack growth rate, is used to calculate the amount of crack growth at each crack front node. However, if there is any nodal point where the amount of crack growth exceeds the maximum crack growth length set by the user, the time increment is automatically reduced so that the maximum crack growth along the crack front does not exceed the specified crack growth limit. This method was employed to ensure that no unrealistic jumps occurred in the crack growth calculations.

PROBLEM FORMULATION AND METHOD OF SOLUTION

One typical DMWs in 3½ inch feeder pipes, for which AFEA has been performed previously, has been selected for the present work. The outer diameter and thickness of the feeder pipe are 101.6 mm (4 inch) and 8 mm (0.315 inch), respectively. Figure 4 shows a schematic illustration of the pipe geometry and the DMW. The weld region was chosen based on metallurgical examinations to have an average weld width of 8.35 mm (0.329 inch). Due to geometric symmetry, half of the feeder has been modeled using regular C3D8 brick element, with total 40,000 elements shown in Figure 1(b). A single postulated

circumferential ID surface crack was placed in the weld center shown in Figure 5. The postulated initial crack takes a quarter of an elliptic shape. Two crack lengths were considered (Case 1: $2c/a = 5.79$, and Case 2: $2c/a = 11.58$ where $2c$ is the initial total ID crack length, $2c/a$ is the so called crack aspect ratio). The selection of the initial flaw size is arbitrary and not based on any actual DMW crack profiles. Modelling growth from only single initial crack instead of multiple cracks is chosen considering the most likely scenario for crack initiation in the welds. Crack initiation is most likely to occur at the most severe weld flaw or at the start/stop region if flaws are present, where the peak axial residual stress at the start/stop region is almost two times of the axial residual stress in other locations along the circumference. Axial cracking has not been considered in this work due to its low safety consequence. The maximum length of axial crack is limited to the weld width (including alloy 600) so that the leakage would be of a limit amount (may not be detectable) and it is unlikely that such a short axial crack would be unstable under any design transients.

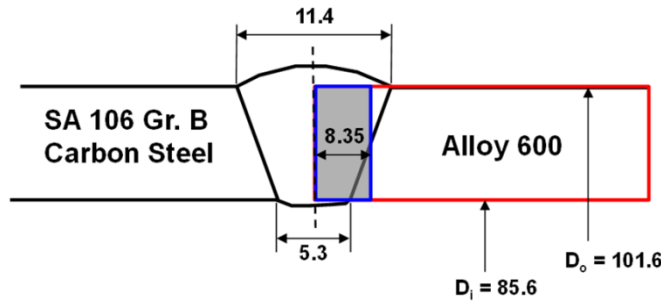


Figure 4 Schematic representation of DMW in feeder pipe (unit: mm)

The material properties of alloy 600 at 312°C are as follows: Young's modulus, $E = 197,397$ MPa (28,630 ksi), Poisson's ratio, $\nu = 0.31$, and thermal expansion coefficient, $\alpha = 4.715 \times 10^{-6}$ mm/mm/°C. It is to be noted that the XFEM results for PWSCC crack growth predictions are independent of material properties since PWSCC crack growth predictions are based on K_I values obtained from XFEM.

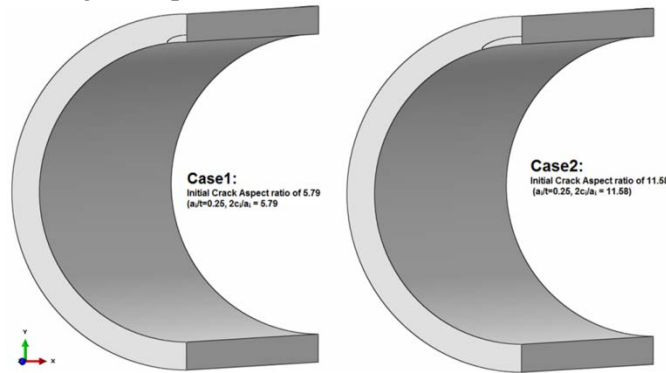


Figure 5 Postulated initial semi-elliptical ID surface cracks with XFEM

Table 1 Selected normal operating loads for Candu feeder pipe

Normal operating temperature °C (°F)	Internal pressure MPa (ksi)	Axial tension* kN (kip)	Bending moment kN-m (kip-inch)
312 (593.6)	10.3 (1.494)	60.610 (13.626)	0.266 (2.354)

*Includes tension due to internal pressure (end-cap effect).

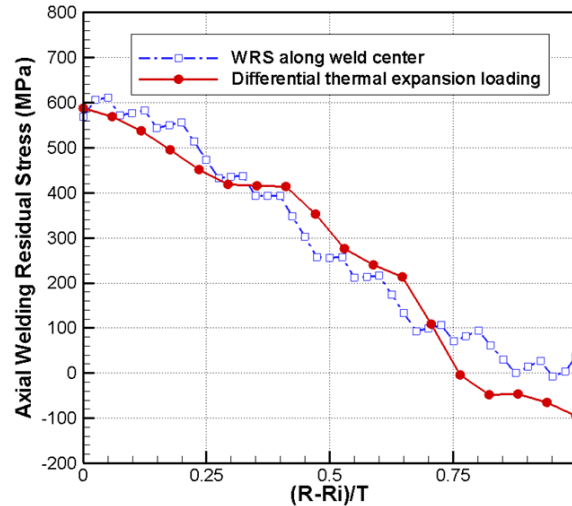


Figure 6 Axial WRS through the thickness of the weld along the weld center

The normal operating loads of DWM feeder pipes are summarized in Table 1 and applied to the model through ABAQUS user subroutine DLOAD. The WRS for the feeder pipe DMW was obtained from the weld simulation results, which were validated by the measurements using neutron diffraction and X-ray diffraction techniques. The highest through-thickness weld residual stress in the weld center was chosen as shown in Figure 6. This represents the WRS case that would cause the quickest crack growth of an initial surface crack to a through-wall crack in each of those locations and hence represents a conservative estimate of the time to leakage. The axial WRS is applied through ABAQUS user subroutine UTEMP.

RESULTS AND DISCUSSIONS

Crack Propagation

Using the normal operating conditions and the WRS described in the previous section, circumferential-crack growth was performed within the elastic range. The initial crack depth was fixed to 25% of the thickness ($a/t=0.25$, where a is the initial crack depth and t is the thickness). Two crack lengths were considered (Case 1: $2c/a = 5.79$, and Case 2: $2c/a = 11.58$ where $2c$ is the initial total ID crack length). Figure 5 shows the two initial surface cracks defined by XFEM. The XFEM was conducted until the through-wall crack front reached to arbitrary 180° around the circumference of the DMW region, which is expected to be much longer than the critical crack size.

Figure 7 shows Case 1 surface crack progression until the initial leakage occurs, while Figure 8 shows the through-wall crack growth results of Case 1. The initial semi-elliptical surface crack formed an arbitrary surface crack as it grew through the wall. The time to incipient leakage with XFEM was 0.42 years with an ID crack length of 44° . After that, the crack penetrated through the wall. The crack front near the OD surface grew much faster than the crack front near the ID surface. As a result, the crack grew to a nearly idealized through-wall crack after 0.705 years. In comparison with AFEA results, the predicted crack profiles are very close to each other before the through-wall crack has been reached. XFEM predicted the incipient leakage at 0.42 year, while AFEA predicts 0.48 year. The through-wall crack growth shows a bit of difference in crack profiles. XFEM predicts a relatively high growth rate than AFEA does. This difference could be due to different approaches in calculating the stress intensity factor and different smooth techniques applied.

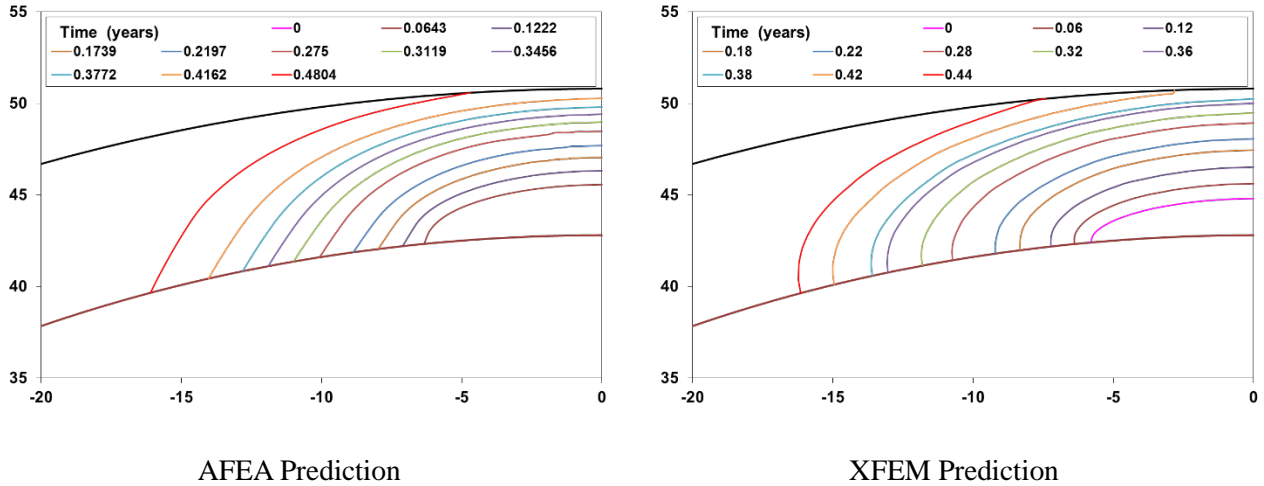


Figure 7 Surface crack growth Case 1: initial crack aspect ratio of 5.79 ($a_i/t=0.25$, $2c_i/a_i = 5.79$, unit: mm)

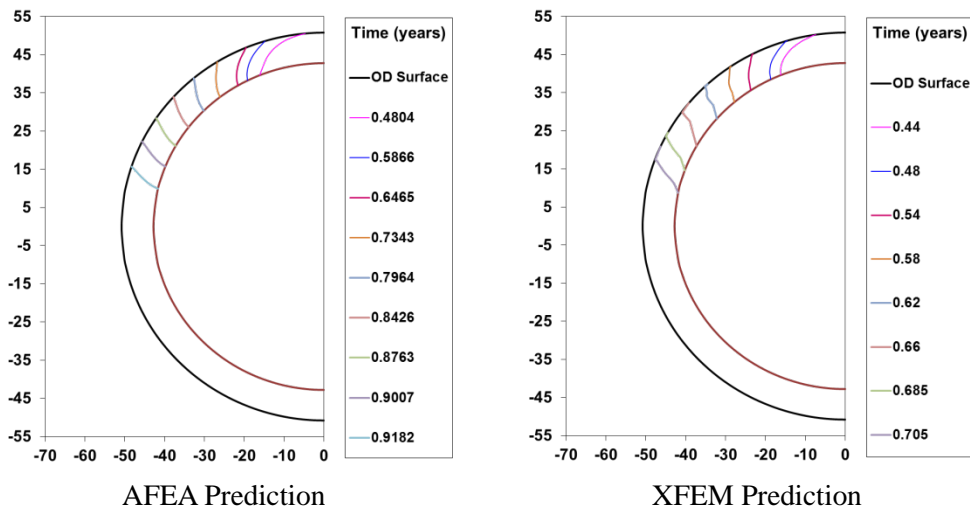


Figure 8 Through-wall crack growth Case 1: initial crack aspect ratio of 5.79 ($a_i/t=0.25$, $2c_i/a_i = 5.79$, unit: mm)

Figure 9 and Figure 10 shows the crack growth results for Case 2: a longer initial surface crack length ($2c/a = 11.58$). The trend in the crack growth for this long surface crack was similar to the results of the short initial surface crack ($2c/a = 5.79$). The time to incipient leakage for this long surface crack predicted by XFEM was 0.34 year, in comparison with 0.3365 years by AFEA. Similarly, XFEM predicts a bit faster crack growth than AFEA during the through-wall propagation.

Although, the simulations for Case 2 started off with twice the ID surface crack length simulated for Case 1, the difference was almost negligible by the time the initial surface crack penetrates the wall to become through wall crack. From this sensitivity study, it was demonstrated that although the time to incipient leakage was marginally different, both cracks formed a similar shaped leakage crack and subsequently formed a nearly idealized through-wall crack in the later stages of the crack growth. Case 1 and Case 2 results justify the use of an idealized crack profile in the piping test.

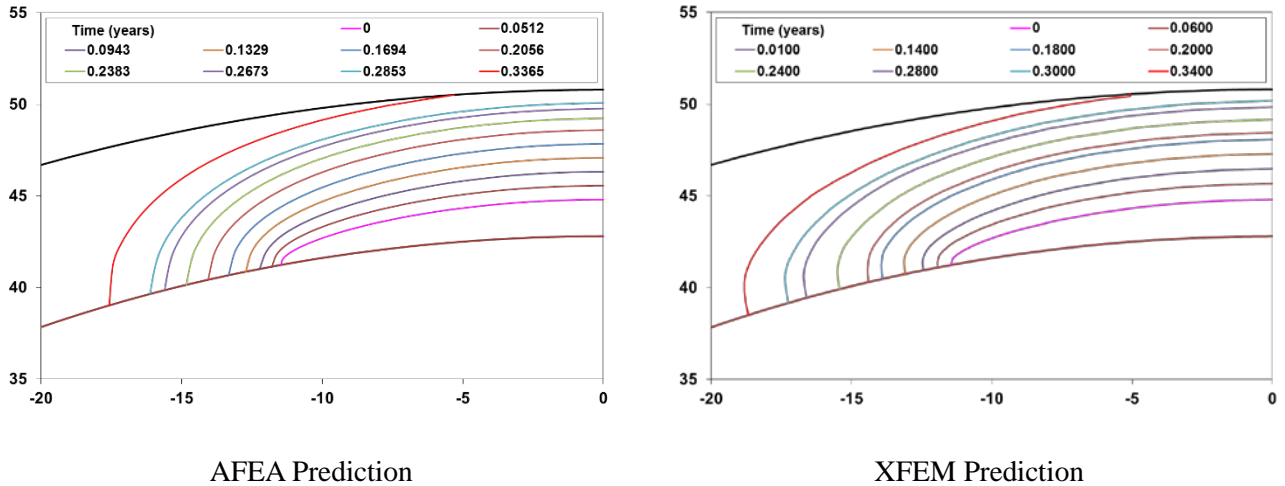


Figure 9 Surface crack growth Case2 – initial crack aspect ratio of 11.58 ($a_i/t=0.25$, $2c_i/a_i = 11.58$, unit: mm), (a) AFEA predicted results; (b) XFEM predicted results

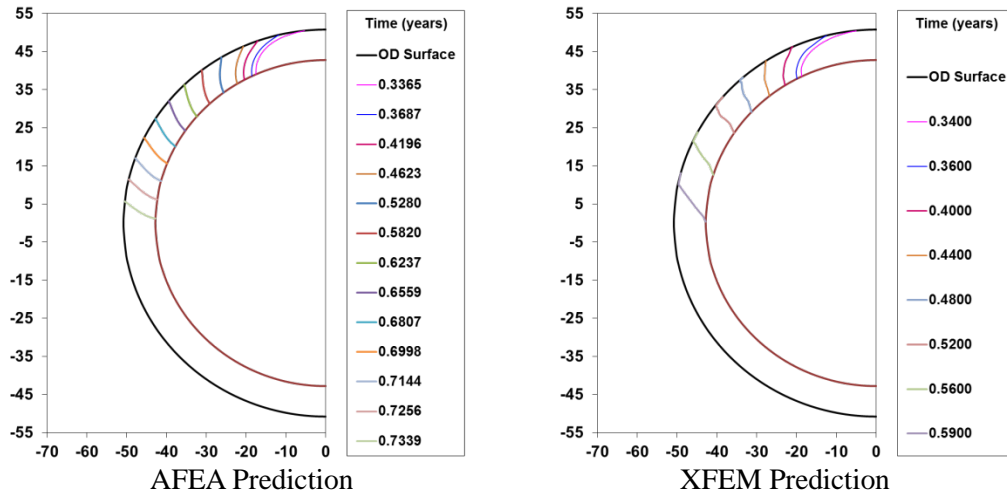


Figure 10 Surface crack growth Case2 – initial crack aspect ratio of 11.58 ($a_i/t=0.25$, $2c_i/a_i = 11.58$, unit: mm), (a) AFEA predicted results; (b) XFEM predicted results.

Leak Rate

Leak rate calculations were performed using the SQUIRT code [11]. The leak rates were calculated using these COD values along with the corresponding OD crack lengths. Figure 11 and Figure 12 show the leak rates estimated from the circumferential through-wall cracks for both Case 1 and Case 2. The time for incipient leakage of short length crack (Case 1) was determined to be 0.42 years by XFEM while the time for incipient leakage was 0.34 years for long length crack (Case 2). From the leak detection point of view, the time for the leak rate of 0.007 kg/s was determined to be 0.36 years for Case 2 and 0.44 years for Case 1.

Both cracks show very a similar leak trend for a given time. However, the long length crack (Case 2) grows much faster growth than the short length crack (Case 1) before changing from surface crack to through wall crack, although operating conditions and WRS are set the same for both cases.

These results prove that the initial crack geometry/profile is an important element in determining the crack growth rate and leak rate in the CANDU feeder pipes.

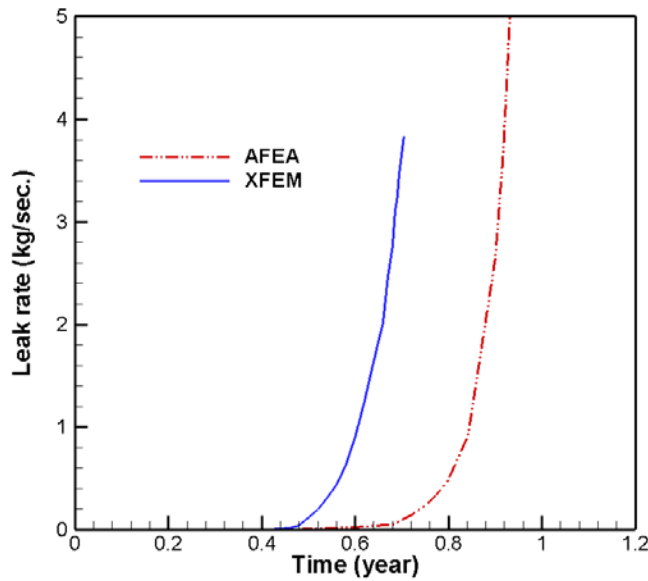


Figure 11 Leak rate predicted by AFEA and XFEM (Case 1).

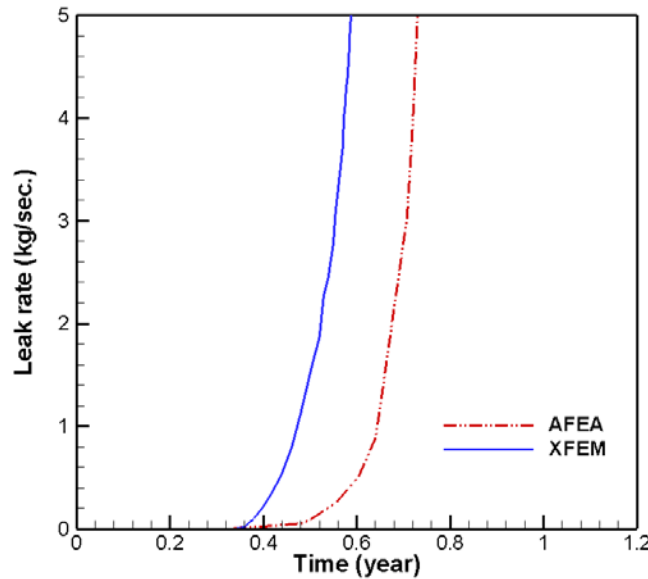


Figure 12 Leak rate predicted by AFEA and XFEM (Case 2).

CONCLUSIONS

In the present work, the extend finite element method (XFEM) approach has been developed through ABAQUS python program to evaluate postulated circumferential PWSCC crack in feeder pipe dissimilar metal welds of CANDU power plants. The comparison of XFEM natural crack growth prediction with the advanced finite element analysis (AFEA, a focused mesh method) shows a good agreement in terms of crack progression from surface crack to through-wall crack and the crack growth rate. This new approach will significantly reduce model build-up efforts for the finite element based crack growth modeling. It also makes 3D arbitrary crack modeling possible.

NOMENCLATURE

AFEA	Advanced Finite Element Analysis
DMW	Dissimilar Metal Weld
ID	Inside Diameter
OD	Outside Diameter
PWSCC	Primary Water Stress Corrosion Cracking
XFEM	Extended Finite Element Method

REFERENCES

- [1] N.-S. Huh, D.-J. Shim, Y.-S. Yoo, S. Choi and K-B. Park, *Estimates of elastic crack opening displacements of slanted through-wall cracks in plates and cylinder*, Journal of Pressure Vessel Technology, (2010), Vol. 132/021401-1.
- [2] Y.-S. Yoo, *Crack opening displacement of circumferential through-wall cracked cylinders subjected to tensile and through-wall bending loads*, Nuclear Engineering and Design, (2004), 229(2):123-138.
- [3] Y.J. Kim and N.S. Huh, *Enhanced reference stress-based J and crack opening displacement estimation method for leak-before-break analysis and comparison with GE.EPRI method*, Fatigue & Fracture of Engineering Materials & Structures, (2001), 24(4):243 – 254.
- [4] S Rahman, F.W Brust, N Ghadiali and G.M Wilkowski, *Crack-opening-area analyses for circumferential through-wall cracks in pipes—Part II: model validation*, International Journal of Pressure Vessels and Piping, (1998), 75(5-75):375-396.
- [5] Y.-J. Kim, N.-S. Huh, Y.-J. Kim, *Quantification of pressure-induced hoop stress effect on fracture analysis of circumferential through-wall cracked pipes*, Engineering Fracture Mechanics, (2002), 69(11):1249-1267.
- [6] Y.-J. Kim, N.-S. Huh and Y.-J. Kim, *Reference stress based elastic–plastic fracture analysis for circumferential through-wall cracked pipes under combined tension and bending*, Engineering Fracture Mechanics, (2002), 69(3):367-388.
- [7] ABAQUS User Manual, Version 6-13, 2013.
- [8] Materials Reliability Program MRP-115, *Crack Growth Rates for Evaluating Primary Water Stress Corrosion Cracking (PWSCC) of Alloy 82, 182, and 132 Welds*, EPRI report number 1006696, Palo Alto, CA: 2004.
- [9] D.L. Rudland, D.J. Shim, T. Zhang, G. Wilkowski, *Implications of Wolf Creek Indications – Final Report, Program final report to the NRC*, ADAMS file number ML072470394, 2007.
- [10] Materials Reliability Program MRP-216, Rev. 1, *Advanced FEA Evaluation of Growth of Postulated Circumferential PWSCC Flaws in Pressurizer Nozzle Dissimilar Metal Welds*, EPRI report number 1015383, Palo Alto, CA: 2007.
- [11] User's Guide for SQUIRT (Windows Version 1.1), Battelle Memorial Institute, 2003 March.